Mon. Not. R. Astron. Soc. **375,** 417–424 (2007) doi:10.1111/j.1365-2966.2006.11289.x

Bulk Comptonization spectra in blazars

A. Celotti,[1⋆] G. Ghisellini[2⋆] and A. C. Fabian[3⋆]
[1]*SISSA/ISAS, Via Beirut 2-4, I-34014 Trieste, Italy*
[2]*INAF, Osservatorio Astronomico di Brera, via E. Bianchi 46, I-23807 Merate (LC), Italy*
[3]*Institute of Astronomy, Madingley Road, Cambridge CB3 0HA*

Accepted 2006 November 6. Received 2006 October 11; in original form 2006 June 12

ABSTRACT

We study the time-dependent spectra produced via the bulk Compton process by a cold, relativistic shell of plasma moving (and accelerating) along the jet of a blazar, scattering on external photons emitted by the accretion disc and reprocessed in the broad-line region (BLR). The bulk Comptonization of disc photons is shown to yield a spectral component contributing in the far-ultraviolet band, and would then be currently unobservable. On the contrary, the bulk Comptonization of broad-line photons may yield a significant feature in the soft X-ray band. Such a feature is time-dependent and transient, and dominates over the non-thermal continuum only when: (i) the dissipation occurs close to, but within, the BLR; and (ii) other competing processes, like the synchrotron self-Compton emission, yield a negligible flux in the X-ray band. The presence of a bulk Compton component may account for the X-ray properties of high-redshift blazars that show a flattening (and possibly a hump) in the soft X-rays, previously interpreted as due to intrinsic absorption. We discuss why the conditions leading to a detectable bulk Compton feature might be met only occasionally in high-redshift blazars, concluding that the absence of such a feature in the spectra of most blazars should not be taken as evidence against matter-dominated relativistic jets. The detection of such a component carries key information on the bulk Lorentz factor and kinetic energy associated to (cold) leptons.

Key words: radiation mechanisms: non-thermal – scattering – quasars: general – quasars: individual: GB B1428+4217 – X-rays: general.

1 INTRODUCTION

High-redshift blazars are the most powerful observed radio-loud active galactic nuclei, and among the best candidates to be detected by the forthcoming *GLAST* γ-ray satellite. Recently, one previously unidentified EGRET source has been associated with the blazar Q0906−693 at a redshift 5.47 (Romani et al. 2004). Its spectral energy distribution (SED) resembles the predictions of the proposed 'blazar sequence' (Fossati et al. 1998; Ghisellini et al. 1998), namely the presence of two broad peaks in the millimetre–far-infrared and the MeV–GeV bands, with the high-energy component strongly dominating the energy output. Furthermore, there are now half a dozen blazars at $z > 4$, yet undetected in the MeV–GeV band, but observed in the X-ray band with large-area instruments (i.e. *XMM–Newton*, see Yuan et al. 2006). All of them exhibit a flat (i.e. rising in νF_ν) spectrum, indicating the energetic dominance of a spectral component peaking at high frequencies. The inferred apparent luminosities reach $>10^{49}$ erg s^{-1}, yet the intrinsic ones (i.e. corrected for the effect of relativistic beaming) are likely to be only a minor fraction of the jet power which energizes the radio lobes.

Despite the theoretical advances following the discovery of the radiatively dominant γ-ray emission in blazars, and more than 30 yr after the discovery of superluminal motion in 3C 273 (Cohen et al. 1971; Whitney et al. 1971), we are still unable to pin down the acceleration and collimation mechanism(s) and establish whether the energy carried in jets is mainly in the form of Poynting flux or kinetic energy of matter and how this might depend on the distance from the powering source (see the arguments presented by Blandford 2002 and Lyutikov 2003 in favour of electromagnetically dominated jets, and Sikora et al. 2005 for a discussion of matter versus magnetic jets).

One of the proposed diagnostics on the issue of jet composition (e.g. Sikora & Madejski 2000) is based on the spectral signature expected from a matter-dominated jet, in the form of an excess of emission at around 1 keV, due to the bulk Comptonization by cold leptons of the radiation fields produced by the accretion disc and/or reprocessed in the broad-line region (BLR). This process, first suggested by Begelman & Sikora (1987), was then considered by

⋆E-mail: celotti@sissa.it (AC); gabriele@merate.mi.astro.it (GG); acf@ast.cam.ac.uk (ACF)

Sikora, Begelman & Rees (1994) and Sikora et al. (1997). Moderski et al. (2004) proposed that such a process can generate a soft X-ray precursor in the light curve of blazars.

No evidence for bulk Comptonization features have been detected so far, leading to upper limits on the jet matter content (see the above-mentioned references). However, there is increasing recent evidence that the X-ray spectrum of some high-redshift blazars shows a flattening towards low X-ray energies and possibly a hump. The favoured interpretation so far has been the presence of intrinsic absorption by warm material, but alternative explanations are viable (see Fabian et al. 2001b; Worsley et al. 2004). In particular, it is possible that for the first time we are observing the signature of the bulk Comptonization process.

This motivates this work which concentrates on the (time-dependent) detailed shape of the bulk Compton spectrum to assess this hypothesis against available and future data, under reasonable assumptions about the presence of ambient seed photons and the bulk acceleration of the plasma in the jet. Future X-ray missions could provide variability as well as polarimetric information in the X-ray band, the latter being a further valuable tool to single out emission via bulk Comptonization among competing radiation processes (Begelman & Sikora 1987), such as synchrotron self-Compton (SSC) (Celotti & Matt 1994), and external Compton (Poutanen 1994).

2 MODEL ASSUMPTIONS

We consider a shell comprising N cold (i.e. non-relativistic) leptons moving along a jet, accelerating up to a saturation speed. During propagation, the leptons scatter ambient photons, originating in a (standard) radiatively efficient accretion disc and reprocessed in the gas clouds forming the BLR, as expected in powerful quasars. In the following, we detail the assumptions made in this scenario.

2.1 Plasma dynamics

The plasma dynamics and, in particular, the dependence of the jet velocity on distance z from the power source, is not known. Modelling of magnetically accelerated flows leads to relatively slow acceleration (e.g. Begelman & Li 1994), before the flows reach an asymptotic speed. Here, we parametrize the acceleration in terms of the bulk Lorentz factor, Γ, increasing with distance (i.e. the height above the disc) as

$$\Gamma(z) = \Gamma_0 \left(\frac{z}{z_0}\right)^a \tag{1}$$

up to a maximum value $\Gamma_{\max}$, beyond which $\Gamma = \Gamma_{\max}$. The initial bulk Lorentz factor, formally a free parameter, will be considered to be 1, unless otherwise specified. The initial height z_0 (corresponding to the typical distance where acceleration sets in) will be taken of the same order as the inner accretion radius r_0. To simplify the notation, we hereafter set $\Gamma = \Gamma(z)$ and $\beta = \beta(z) = (\Gamma^2 - 1)^{1/2}/\Gamma$.

2.2 Scattering of radiation from the accretion disc

To model the radiation produced by the accretion disc, we simply consider the surface (multicolour blackbody) temperature profile for a Shakura & Sunyaev (1973) disc:

$$T_{\rm D}(r) \propto M_{\rm BH}^{-1/2} \dot{M}^{1/4} r^{-3/4} \left[1 - \left(\frac{6r_{\rm g}}{r}\right)^{1/2}\right]^{1/4}, \tag{2}$$

where r is the radial disc coordinate, $r_{\rm g} = GM_{\rm BH}/c^2$ is the gravitational radius, $M_{\rm BH}$ is the central black hole mass and $\dot{M}$ is the mass-accretion rate.

At a given height z, the bolometric radiation energy density produced by a 'ring' of the accretion disc, as seen in the lab frame, corresponds to

$$\frac{{\rm d}U(z)}{{\rm d}r} = \frac{2\pi r B(T_{\rm D}) \cos\theta}{c(z^2 + r^2)}. \tag{3}$$

$B(T_{\rm D}) = \sigma_{\rm SB} T_{\rm D}^4/\pi$ represents the frequency-integrated blackbody intensity, $\sigma_{\rm SB}$ is the Stefan–Boltzmann constant, and $\cos\,\theta = [1 + (r/z)^2]^{-1/2}$, θ being the angle between the position z along the jet and the emitting ring of the disc.

In the comoving (primed) frame of the shell, this radiation energy density is given by

$$\frac{{\rm d}U'(z)}{{\rm d}r} = \Gamma^2(1 - \beta\cos\theta)^2 \frac{{\rm d}U(z)}{{\rm d}r}. \tag{4}$$

We assume that the scattering process is isotropic, that is, we neglect the angle dependence of the differential Thomson cross-section, by setting ${\rm d}\sigma/{\rm d}\Omega = \sigma_{\rm T}/(4\pi)$. Thus, for an optically thin shell (see Section 2.5), each electron scatters a fraction $\sigma_{\rm T}$ of this radiation energy density, re-isotropizing it in the comoving frame. For N free and cold electrons, the scattered radiation (at a given z) corresponds to a bolometric luminosity (in the comoving frame)

$$\frac{{\rm d}L'(z)}{{\rm d}r} = \sigma_{\rm T} c N \frac{{\rm d}U'(z)}{{\rm d}r}. \tag{5}$$

An observer located at an angle $\theta_{\rm V}$ with respect to the jet axis will receive a power

$$\frac{{\rm d}L_{\rm obs}(z)}{{\rm d}r} = \frac{1}{[\Gamma(1 - \beta\cos\theta_{\rm V})]^4} \frac{{\rm d}L'(z)}{{\rm d}r} \equiv \delta^4(z) \frac{{\rm d}L'(z)}{{\rm d}r}, \tag{6}$$

where $\delta = \Gamma^{-1}(1 - \beta\,\cos\theta_{\rm V})^{-1}$ defines the relativistic Doppler factor. In terms of the spectrum, the observed radiation will still have a blackbody frequency distribution, corresponding to a transformed temperature:

$$T_{\rm D,obs}(r, z) = T_{\rm D}(r) \frac{1 - \beta\cos\theta}{1 - \beta\cos\theta_{\rm V}}. \tag{7}$$

Given the total luminosity (equation 6) and spectrum (equation 7), the observed spectrum can be normalized by setting

$$\frac{{\rm d}L_{\rm obs}(z, \nu)}{{\rm d}r} = A \frac{2h}{c^2} \frac{\nu^3}{\exp(h\nu/kT_{\rm D,obs}) - 1}, \tag{8}$$

$$A = \frac{2\pi\sigma_{\rm T} N r \cos\theta}{z^2 + r^2} \frac{1}{[\Gamma(1 - \beta\cos\theta)]^2}. \tag{9}$$

The observed power emitted at each z can be simply obtained by integrating over the disc radii r, between r_0 and an outer disc radius (see Section 2.5).

In the following, we will also consider the time-integrated spectrum, as measured by the observer over an (integration) time $t_{\rm obs}$, given by

$${\rm d}t_{\rm obs} = \frac{{\rm d}z}{\beta c}(1 - \beta\cos\theta_{\rm V}), \tag{10}$$

leading to

$$t_{\rm obs} = \int_{z_0}^{z} \frac{{\rm d}z'}{\beta c}(1 - \beta\cos\theta_{\rm V}). \tag{11}$$

2.3 Scattering of broad-line photons

Besides the photons directly originating in the disc, a significant contribution to the soft photon field can come from disc photons reprocessed by the gas permeating the BLR (Sikora et al. 1994). We account for this contribution assuming that the photon energy distribution follows a blackbody spectrum peaking at the frequency of the Lyman α (Lyα) hydrogen line, $\nu_{\rm Ly\alpha} = 2.47 \times 10^{15}$ Hz. This matches the shape of this external radiation component in a restricted energy range around the Lyα line, as seen in the comoving frame.

In fact for BLR clouds distributed in two semi-spherical shells (one for each side of the accretion disc), any monochromatic line is seen, in the comoving frame, within a narrow cone of semi-aperture angle $1/\Gamma$ along the jet velocity direction. Accordingly, such photons are blueshifted by a factor ranging from Γ (photons from the border of the cone) to 2Γ (photons head-on). In this (admittedly narrow) frequency range, a monochromatic line transforms into a spectrum $\propto \nu_{\rm obs}{}^2$. Although the Ly$\alpha$ line represents the most important contribution of the BLR seed photons, the entire spectrum produced by the BLR is more complex (see Tavecchio et al., in preparation). Here, we stress that the blackbody assumption represents well the more complex SED from the BLR.

Thus, we set an equivalent temperature of the BLR spectrum:

$$T_{\rm BLR} \equiv \frac{h\nu_{\rm Ly\alpha}}{2.8k} \sim 4.23 \times 10^4\,{\rm K}. \quad (12)$$

In the shell comoving frame, this temperature is seen blueshifted by a factor $\sim\Gamma$, while, after scattering, the transformation in the observer frame introduces an additional blueshift, corresponding to a factor δ: therefore $T_{\rm BLR,obs} \sim \Gamma\delta T_{\rm BLR}$.

The bolometric luminosity resulting from the scattering of BLR photons, at a given distance z, is given by

$$L_{\rm BLR,obs}(z) = \sigma_{\rm T} c N U_{\rm BLR} \Gamma^2 \delta^4, \quad (13)$$

where $U_{\rm BLR}$ is the energy density of BLR photons, which is considered constant within the typical distance of the BLR, defined by a radius $R_{\rm BLR}$. For a luminosity, $L_{\rm BLR}$, of broad-line photons, the observed spectrum will have a blackbody shape, corresponding to the temperature $T_{\rm BLR,obs}$:

$$L_{\rm BLR,obs}(z,\nu) = \frac{2h}{c^2}\,\frac{\nu^3}{\exp(h\nu/kT_{\rm BLR,obs})-1} \times \frac{\sigma_{\rm T} N L_{\rm BLR}}{4\sigma_{\rm SB} R_{\rm BLR}^2 T_{\rm BLR}^4 \Gamma^2}, \quad (14)$$

which corresponds to the integrated luminosity given by equation (13).

2.4 Disc versus broad-line photons

Since the highest temperature is reached in the innermost parts of the accretion disc, the angle between the energetic disc photons and the moving shell is typically small. It is relatively large only in the vicinity of the disc, but there the shell has not yet reached high bulk Lorentz factors. As a consequence (see equation 7), the observed typical frequency of the scattered disc photons will not increase much (for $\theta \sim 0$ and $\theta_{\rm v} \sim \beta$ such photons are even redshifted).

On the contrary, photons from the BLR are always seen head-on, and as such are maximally blueshifted (i.e. by the factor $\Gamma\delta$). For this reason (as shown below), it will be this bulk Compton component which can provide a relevant contribution in the X-ray spectrum of powerful blazars.

2.5 Model parameters

In the following, we quantitatively specify the choice of model parameters adopted in the spectral calculations presented in Section 3.

(i) *Disc luminosity.* For powerful blazars, we assume a typical black hole mass $M_{\rm BH} = 10^9 M_9\ {\rm M}_\odot$ and a disc accretion rate close to the Eddington one. Therefore,

$$L_{\rm disc} \sim L_{\rm Edd} \sim 10^{47} M_9\ {\rm erg\ s^{-1}}, \quad (15)$$

and the typical sizes of the inner accretion disc and jet are assumed $z_0 = r_0 = 6\,r_{\rm g}$. The outer accretion disc radius is set to $10^4 r_{\rm g}$.

(ii) *Broad-line radiation.* We model the BLR as a thin spherical shell at a distance $R_{\rm BLR}$. The disc radiation reprocessed by clouds in the BLR is assumed to have a bolometric luminosity $L_{\rm BLR} = 0.1\,L_{\rm disc}$.

It should be noted that the BLR may not be the only contributor to seed photons, besides those directly from the accretion disc. A molecular torus (emitting infrared photons; e.g. Blazejowski et al. 2004), and intracloud plasma (scattering and isotropizing both disc and beamed synchrotron jet radiation; e.g. Ghisellini & Madau 1996) may also provide soft photons. However, we neglect such components here, as their contribution is very uncertain.

(iii) *Number of electrons.* We consider a shell of plasma, of some initial size equal to the inner size of the accretion disc, r_0. As a first-order estimate of how many particles can be present in such a shell, we consider the number of *relativistic* electrons needed to originate the radiation dominating the SED (i.e. produced in the jet regions where most of the dissipation occurs) and, assuming that the total number of particles is conserved, we treat it as a *lower limit* to the total number of electrons present in the shell.

This limit is clearly model-dependent. We will adopt the most common interpretation that the high-energy radiation in the spectrum of powerful blazars is produced via inverse Compton emission of a relativistic distribution of leptons on the external photon fields discussed in Sections 2.2 and 2.3. In this scenario, the inferred number density of relativistic particles relies on estimates of the magnetic field and seed photon energy density required to give raise to the observed luminosity. On the other hand, these quantities are quite tightly constrained by fitting the whole SED – both the synchrotron and the inverse Compton components. Furthermore for powerful blazars, the electron distribution is basically in the complete cooling regime (namely, electrons of all energies cool within a light crossing time), which constrains the low-energy particle end.

For a reference value of $N = 10^{54} N_{54}$ particles (see Section 3), which initially occupy a volume of typical size $r_0 = f\,2r_{\rm g}$ ($2r_{\rm g}$ being the Schwarzschild radius), the corresponding initial optical depth is $\tau_0 \equiv \sigma_{\rm T} r_0 (N/r_0^3) \sim 7.4 N_{54}/(fM_9)^2$. At the base of the jet, the shell can be optically thick for scattering (depending on f): in the calculations, we rescale the bulk Compton emission by the factor $\max(1, \tau)$, which accounts for the reduction in the scattered flux when $\tau > 1$ (self-shadowing). However, for a conical jet, the region rapidly becomes transparent as $\tau \propto z^{-2}$, independently of the shell width. After transparency is reached, all electrons contribute to the emission and the process becomes largely independent of the specific geometry (shell or spherical), and the expressions given in Section 2.4 are appropriate.

(iv) *Plasma dynamics.* As mentioned above, we parametrize the uncertain dynamics as $\Gamma(z) = (z/z_0)^a$. In the following examples, we adopt $a = 1/2$, which, for $\Gamma_{\rm max} \sim 10$, corresponds to reach the asymptotic bulk Lorentz factor at distances $z = z_0 \Gamma_{\rm max}^2$, approximately a few hundreds $r_{\rm g}$. In the context of the internal shock scenario (Rees 1978; Sikora et al. 1994; Ghisellini 1999; Spada et al.

2001), this is approximately the distance where shell–shell collisions take place, that is, where most of the dissipation occurs. For $a = 1$ (i.e. more rapid acceleration), the results are qualitatively the same, but the observed time-evolution is quicker.

3 RESULTS

Fig. 1 shows a sequence of bulk Compton spectra resulting from scattering disc and line photons. The sequence refers to spectra at different times (in the observer frame) from the beginning of the plasma acceleration at $z_0 = 6r_g$. Each spectrum corresponds to the average luminosity received in 3 h of integration time, t_{obs}, again as measured in the rest frame of the source. The acceleration ($\Gamma \propto z^{1/2}$) terminates when $\Gamma_{max} = 15$ is reached. For comparison, the BLR size is $R_{BLR} = 10^{18}$ cm $\sim 10^4 r_g$.

The total number of cold particles is set at $N \sim 10^{53}$, and the observer is located at a viewing angle $\theta_v = 3^\circ$.

The figure shows separately the contribution from scattering of disc (continuous lines) and BLR (dashed lines) photons. For clarity, the top panel shows the evolution of the spectrum in the rising phase of the disc-scattered component (roughly until the Lorentz factor reaches Γ_{max}), while the bottom panel shows its decline.

Such evolution corresponds to the following phases.

(i) At early times, the bulk Lorentz factor is small, with a correspondingly low scattered luminosity, from both disc and line photons. The former component is more prominent as the radiation energy density of the disc photons is larger at small z. The different slope of the disc-scattered radiation with respect to the multicolour blackbody is due to the dilution of photons produced at larger disc radii, weakly contributing to the total energy density.

(ii) As the jet accelerates (before reaching Γ_{max}), the BLR-scattered component increases more rapidly than the disc-scattered one. This is because the radiation energy density of the BLR photons is constant for a stationary observer inside it, but increases like Γ^2 in the shell comoving frame. The radiation energy density produced by the inner disc, instead, decreases for a stationary observer, and even more so in the shell frame (since the photon directions form small angles with respect to the shell velocity). Only photons produced at large disc radii are blueshifted, and make up the dominant part of the disc radiation energy density.

(iii) When the shell reaches its maximum Lorentz factor (at $t_{obs} \sim 21$ h), it is already relatively far from the disc. In the comoving frame, a larger and larger portion of the disc is seen at small angles (i.e. in the comoving frame photons are seen redshifted).

Correspondingly, the disc-scattered radiation intensity decreases (bottom panel of Fig. 1), while the BLR line-scattered component remains constant and dominates.

(iv) As mentioned in Section 2.4, the typical energies of the disc and BLR line scattered components are different. The disc-scattered hump peaks in the far-ultraviolet (far-UV), in the spectral region currently most difficult to observe. This is because energetic disc photons reach the shell at small angles, except at very early times when, however, the Lorentz factor is still low. Therefore, they are not significantly boosted. Line photons, instead, always intercept the shell head-on (in the comoving frame), and thus are maximally boosted. The peak frequency of this component depends only on the value of Γ that the shell has at a given z (and, of course, on the viewing angle).

To investigate the last item better, which is crucial in assessing the detectability of bulk Compton emission, we show in Fig. 2 the

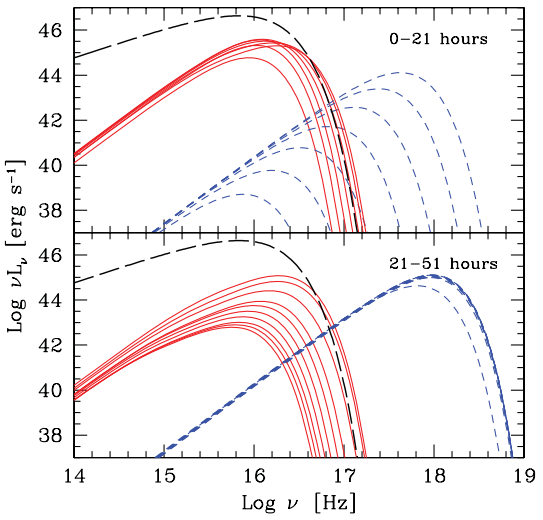

Figure 1. Temporal evolution of the bulk Compton spectrum. Long dashed line: accretion disc spectrum. Solid lines: bulk Compton spectra from scattered disc photons. Dashed lines: bulk Compton spectra from scattered broad-line photons. Each spectrum corresponds to the average luminosity, assuming 3 h of integration time, produced by the shell as it moves from z_0 to the BLR, assumed to be at $R_{BLR} = 10^{18}$ cm. The top panel shows the evolution for the first 21 h (observer time) during which the contribution from bulk Comptonization of disc photons increases; the bottom panel corresponds to the time-interval between 21 and 51 h, during which the same component decreases in flux. Note that the luminosity and spectrum from the bulk Comptonization of BLR photons remain constant after ~21 h (bottom panel), corresponding to the fact that Γ has reached its maximum value.

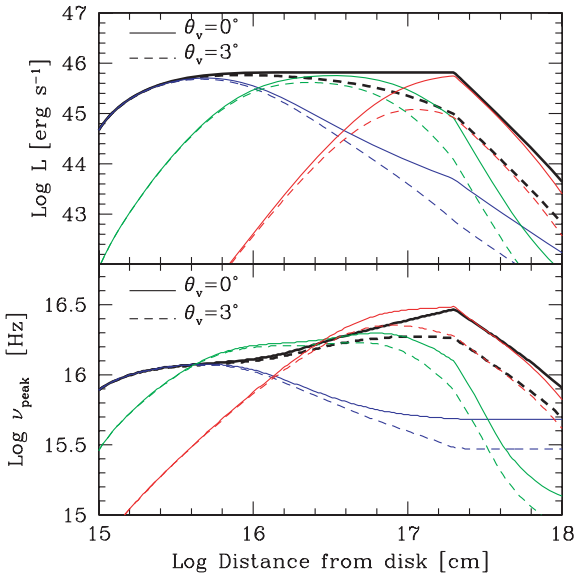

Figure 2. The bolometric bulk Compton luminosity from the scattering of disc photons (top panel) and the frequency peak of this component (bottom panel) as a function of the height of the shell above the disc, z. Broad-line photons are neglected here. The thick (black) lines show the contribution from soft photons produced in the entire disc, while the thin lines represent, respectively, the contribution from 6–60r_g (blue); 60–600r_g (green) and 600–6000r_g (red). Note that the three regions of the disc similarly contribute to the total luminosity. The solid and dashed lines correspond to viewing angles $\theta_v = 0^\circ$ and 3°, respectively. We assumed $L_{disc} = 10^{47}$ erg s^{-1}, $M_{BH} = 10^9$ M$_\odot$.

bolometric luminosity and the peak frequency of the disc-scattered spectrum as a function of the shell–disc distance, z. The solid and dashed lines correspond to $\theta_v = 0^\circ$ and 3°, respectively. The contribution of seed photons from the inner (6–$60r_g$), central (60–$600r_g$) and outer (600–$6000r_g$) parts of the disc is shown separately: the inner part is relevant only when the shell is close to the disc, while the other part mostly contributes when the shell moves beyond a few ($\sim$10) r_g. The curves change behaviour when Γ reaches Γ_{max} (or $z > R_{BLR}$), which in this particular example occurs at $z \sim 2 \times 10^{17}$ cm.

3.1 The case of GB B1428+4217

To illustrate the possible relevance of the bulk Compton process for the interpretation of the X-ray spectra of blazars, which motivates this work, we consider the case of GB B1428+4217, a powerful blazar at redshift $z = 4.72$. This is one of the best-studied high-redshift ($z > 4$) blazars, the spectrum of which has been observed in X-rays by *ROSAT* (Boller et al. 2000), *BeppoSAX* (Fabian et al. 2001a) and *XMM–Newton* (Worsley et al. 2004, 2006). These observations showed that the X-ray spectra flatten towards low energies with respect to a higher-energy power law. This behaviour has been interpreted as likely due to (warm) absorbing material (with columns exceeding 10^{22} cm^{-2}). Alternative interpretations are, however, possible (Fabian et al. 2001b): a flattening of the low-energy part of an inverse Compton component could be due to a low energy cut-off in the electron population and/or a sharply peaked soft (seed) photon distribution. The sharpness of the X-ray break (occurring over a range of only a few keV in the rest frame) is, however, difficult to explain within these models.

Here, we consider the possibility that the flattening and (possibly) a hump in the soft X-ray spectrum (see Worsley et al. 2004; Yuan et al. 2005) reveal the presence of emission via bulk Comptonization. For this specific example, we consider the parameters which allow us to reproduce the high-energy spectral component on the basis of the external inverse Compton process (e.g. in Ghisellini, Celotti & Costamante 2002). The SED can be satisfactorily fitted as emission of a shell with cross-section radius $\sim 2 \times 10^{16}$ cm and width (as measured in the comoving frame) $\Delta R' = 1.2 \times 10^{15}$ cm, moving with a bulk Lorentz factor $\Gamma = 17$. The inferred magnetic field is $B = 11$ G and the (comoving) number density of relativistic particles is $\sim 5.9 \times 10^5$ cm^{-3}, corresponding to a total number of relativistic particles $N_{rel} \sim 8.8 \times 10^{53}$. The observer is at $\theta_v = 3^\circ$.

To account also for the soft X-ray flattening and hump, we assume that again the plasma accelerates from $z_0 = 6r_g$ according to $\Gamma = (z/z_0)^{1/2}$, up to $\Gamma_{max} = 17$. The dynamics of the shell with respect to the observer time corresponds to the case presented in Fig. 3. The disc luminosity is $L_{disc} = 4 \times 10^{47}$ erg s^{-1}, for an $M_{BH} = 4 \times 10^9$ M$_\odot$. The BLR, located at $R_{BLR} = 1.2 \times 10^{18}$ cm, reprocesses 10 per cent of the disc radiation. The resulting spectra are shown in Fig. 4, where we report different X-ray data sets, and optimize the parameters to reproduce the *BeppoSAX* (top panel) and *XMM–Newton* (bottom panel) states.

The overall SED clearly depends on the relative normalization of the relativistic and cold electron distributions. The power-law components in Fig. 4 (dotted lines) extend from the peaks of the two bulk Compton components: this corresponds to a similar number of electrons in the two particle distributions,[1] namely a total number of

[1] For the relativistic particle distribution, we assume $N(\gamma) \propto \gamma^{-(2\alpha+1)}$ extending down to $\gamma_{min} \sim 1$, where α is the spectral index, $L(\nu) \propto \nu^{-\alpha}$.

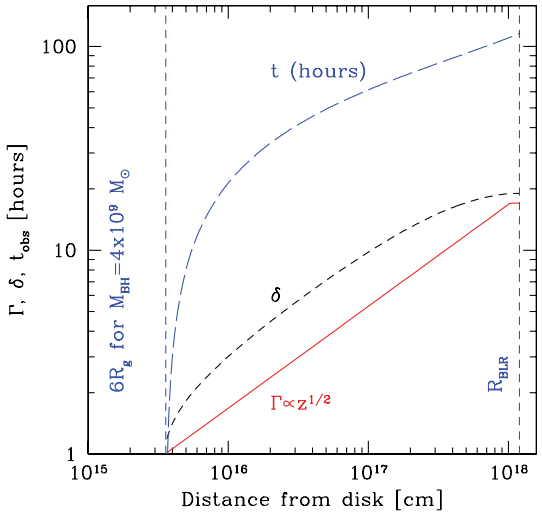

Figure 3. The bulk Lorentz factor Γ, Doppler factor δ, and observed (rest frame) time t_{obs} (the latter expressed in hours), as a function of the location of the shell above the disc. The input parameters are the same as used in the previous case, except for $L_{disc} = 4 \times 10^{47}$ erg s^{-1} (for a black hole of $M_{BH} = 4 \times 10^9$ M$_\odot$); $R_{BLR} = 1.2 \times 10^{18}$ cm; a total number of (cold) particles $N = 8.6 \times 10^{54}$ and a viewing angle $\theta_v = 3^\circ$. The vertical dashed lines correspond to the start of our calculations (i.e. $6r_g$) and the assumed location of the BLR.

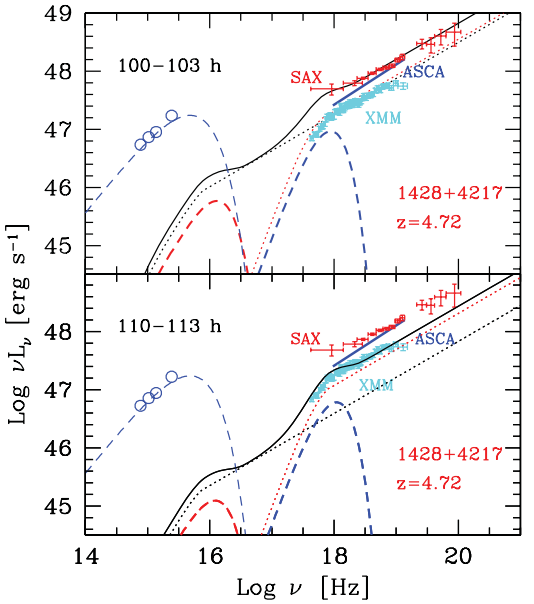

Figure 4. Illustration of how the bulk Compton process can explain some details of the X-ray spectrum of a powerful blazar, GB B1428+4217. The X-ray data are from *BeppoSAX* (red in the online version), *XMM–Newton* (cyan in the online version) and *ASCA* (blue in the online version). The power law is assumed to start from the top of the two Comptonization humps, corresponding to the assumption that a number of leptons similar to those 'cold' are accelerated to relativistic energies and form a power-law distribution extending down to $\gamma_{min} = 1$. Top panel: spectrum predicted during 3 h of exposure time, starting 100 h after the beginning of the acceleration. Bottom panel: the same, but after 110 h. Due to the hardness of the power law, the contribution to the total power law of disc and broad-line photons is almost equal even after 100 h, despite the fact that the bulk Compton hump from disc photons is less powerful than the one from the broad-line photons. All frequencies are in the rest frame of the source.

(cold) particles $N = 4.0\,(1.3) \times 10^{54}$ (for the top and bottom panels, respectively).

The normalizations of the relativistic and cold particle distributions have been assumed to be similar, and the two populations have been considered independently. Clearly, a self-consistent treatment should, in principle, account for the acceleration and cooling processes to determine the relative normalization (in number and energy) as a function of time. The assumption made here corresponds to about half of the particles present at the dissipation site to be accelerated. Alternatively, this could correspond to a situation where all leptons are cold for half of the exposure time, and relativistic for the other half.

The spectra shown in Fig. 4 refer to the average luminosity detected in three hours of integration time (rest frame), starting at $t_1 = 100$ h (top panel) and $t_2 = 110$ h (bottom panel) with respect to the beginning of the acceleration ($z = z_0$). These times correspond to locations of the shell quite close to $R_{\rm BLR}$ (see Fig. 3).

After t_1, the luminosities (νL_ν) of the bulk Compton spectra of disc and line-scattered photons are similar, while at t_2 the contribution from the line photons dominates. In fact, by t_2 the shell has already reached its maximum Lorentz factor, quite far from the inner parts of the disc.

As already shown (see Fig. 1), the bulk Compton spectrum of the disc photons, at all times, peaks in the far-UV, and is thus undetectable. However, its luminosity is highly time-dependent (see the top panel of Fig. 1), exceeding the bulk Compton luminosity off line photons at times $t \lesssim t_1$ (rest frame) for the specific example shown here.

As a consequence, had dissipation – namely acceleration of electrons to relativistic energies – occurred at lower height above the disc, we would have a non-thermal spectrum dominated by the scattering of the disc, not line, photons. This would imply that the X-ray excess due to bulk Compton off the line photons would become undetectable, being exceeded by non-thermal radiation. This can be seen by comparing the spectra in the top and bottom panels of Fig. 4. Early dissipation, however, faces a severe difficulty in accounting for the SED, since the source becomes opaque to the $\gamma - \gamma \rightarrow e^{\pm}$ process. The emission of the created pairs would contribute at frequencies between the two broad peaks of the SED, resulting in an overproduction of X-rays with respect to the observed level (Ghisellini & Madau 1996).

Note that – as shown in Fig. 4 – the power-law continuum from disc-scattered photons dominates over a limited frequency range even if the corresponding bolometric energy density is smaller than that of line-scattered photons. For non-thermal scattered radiation with a hard spectrum ($\alpha < 1$), the typical frequencies of the seed photons are important: disc radiation should not be discarded as a main contributor to the seed photon field, on the basis of its bolometric energy density only (see Dermer & Schlickeiser 1993).

In the observationally interesting X-ray range (i.e. 0.1–10 keV, that translates into 0.5–50 keV rest frame for sources at $z \sim 4$), the spectrum can be approximated as the sum of a power law and a blackbody. The latter component would correspond to a hump in the mid X-ray band, accompanied by a flattening towards soft energies.

The bulk Compton feature is expected to be time-dependent, and generally transient. The necessary conditions for it to be detectable are: (i) dissipation must occur far from the accretion disc, but within and near to the BLR; (ii) the shell should move close to its maximum speed; and (iii) other competing processes, such as SSC, should not dominate over the bulk Compton and external inverse Compton processes (see Section 4).

4 DISCUSSION

We have shown that bulk Comptonization of the radiation from an accretion disc around a supermassive black hole, although important in a bolometric sense, would be currently unobservable, since its spectrum peaks in the far-UV. On the contrary, the bulk Compton process on photons produced in the BLR can give raise to an observable feature which can be represented by a blackbody. The entire (bulk Compton+relativistic Compton) spectral shape, can then be approximated as a blackbody+power law.

The bulk Compton feature is however difficult to detect, even in the most favourable case. First, in general, it can be a transient feature, if the plasma injection or dissipation in the jet is not continuous. Such possibilities are, in general, supported by the strong variability across the electromagnetic spectrum of blazars. Above we mimicked these possibilities assuming that the dissipation region is a shell moving along the jet, thus giving raise to a bulk Compton feature when the shell is close to the BLR. However, it is well possible that a 'cold' component is in fact more continuous. In such a case, the bulk Compton component would correspond to the 'integration' of the spectra shown. Secondly, the radiation has to be strongly beamed, namely the jet has to be highly relativistic and the angle with the line of sight small. A third condition for a bulk Compton feature to be detectable is that other emission processes do not mask it. The most likely component that could hide it is that produced by SSC. It should be noted that the estimated spectrum (see Fig. 4) does not include emission via the SSC process, as this would require to assume – as another free parameter – the relative intensity of the external soft photon and magnetic fields. The SSC could, in principle, provide a significant contribution at the UV and softest X-ray energies even in powerful sources. However, from the observational point of view, the SSC component contributes the least to the X-ray spectrum of the most powerful sources, since among blazars they show the flattest X-ray spectra and the largest 'Compton dominance', that is, the ratio of the high- versus low-energy components increases as the bolometric luminosity does (Fossati et al. 1998). This can be interpreted (Ghisellini et al. 1998) as due to the increased importance of the external seed radiation field relative to the locally produced synchrotron one with increasing source power.

This contrasts with the finding that the radiation energy density of BLR photons decreases or remains constant in higher-luminosity objects, according to the relations reported by Kaspi et al. (2000) and Bentz et al. (2006), respectively. On the other hand, BLR photons might not be the only contributors to the seed field: the BLR clouds themselves and/or some intracloud scattering material can enhance and isotropize beamed synchrotron radiation from the jet, the external radiation (Ghisellini & Madau 1996) and disc radiation (Sikora et al. 1994). The presence and the optical depth of such scattering material could depend on the disc luminosity: more massive outflows or winds from the disc could be favoured at accretion rates near the Eddington one. The emission lines and thermal optical–UV component in high-redshift blazars indeed indicate accretion luminosities close to the Eddington ones even for black hole masses exceeding 10^9 $M_\odot$.

If the Lyα hydrogen line provides most of the seed photon field, the detection of the bulk Compton signature would constitute a powerful diagnostic to estimate the product $\delta\Gamma$. Another independent estimate of Γ or δ, would then allow us to estimate both the jet speed and the viewing angle. For instance, if the source shows superluminal motion with an apparent speed $\beta_{\rm a}$ (and assuming Γ does

not change), we have

$$\Gamma\delta = \frac{\nu_{\rm p}}{\nu_{\rm Ly\alpha}}, \tag{16}$$

$$\beta_{\rm a} = \frac{\beta \sin\theta_{\rm v}}{1-\beta\cos\theta_{\rm v}} \rightarrow \Gamma\delta = \frac{\beta_{\rm a}}{\beta\sin\theta_{\rm v}}, \tag{17}$$

where $\nu_{\rm p}$ is the peak of the bulk Compton spectrum. The above two equations can be solved for $\theta_{\rm v}$ and Γ:

$$\sin\theta_{\rm v} = \frac{\beta_{\rm a}}{\beta}\,\frac{\nu_{\rm Ly\alpha}}{\nu_{\rm p}}, \tag{18}$$

$$\Gamma = \frac{\nu_{\rm p}/\nu_{\rm Ly\alpha}}{\left[(2\nu_{\rm p}/\nu_{\rm Ly\alpha}) - 1 - \beta_{\rm a}^2\right]^{1/2}}. \tag{19}$$

The other key diagnostic which can be inferred from a bulk Compton feature is the kinetic energy associated to the cold scattering material, which is independent of the magnetic field intensity and the filling factor of the scattering plasma.

In the case of GB B1428+4217, the above interpretation of the SED implies $E_{\rm kin} = N\Gamma m_{\rm p}c^2 \sim 10(3.4) \times 10^{53}$ erg, for a proton–electron plasma. If the width of the shell containing this mass is of the order of the initial jet size (in the observer frame, i.e. $\Delta R \sim 6r_g \sim 3.6 \times 10^{15}$ cm), then the corresponding kinetic luminosity is $L_{\rm kin} = E_{\rm kin}c/(6r_{\rm g}) \sim 8.6(2.8) \times 10^{47}$ erg s^{-1}, corresponding to about the luminosity radiated by the accretion disc. $L_{\rm kin}$ is clearly less if there are electron–positron pairs; it should be noted that in the case of a pair-dominated plasma, the jet could be significantly decelerated because of the drag due to the bulk Compton, but even more so when dissipation occurs and also the 'rocket' effect would come into play. Note also that $L_{\rm kin} \propto 1/\Delta R$. ΔR is here a free, unknown parameter and indeed a different assumption on ΔR has been made by Ghisellini et al. (2002). However, despite this uncertainty on $L_{\rm kin}$, the effective $E_{\rm kin}$ is in fact substantially independent of such choice.

Fitting the overall SED would also allow us to estimate the magnetic field intensity and hence the power in Poynting flux. For this purpose, we will examine the X-ray data and SED of powerful, high-redshift blazars with indications of a bulk Compton feature (Fabian et al., in preparation). Interestingly, in agreement with the prediction of this scenario, indications of soft X-ray flattening appear to be connected with the source X-ray luminosity (Yuan et al. 2006).

Future large-area X-ray instruments might even provide time-dependent X-ray spectra from which, in principle, it should be possible to constrain the jet acceleration. Nevertheless, different shells might contribute to the observed spectrum and, thus, the deconvolution from X-ray variability to plasma acceleration might be much more complex than that outlined here.

5 CONCLUSIONS

The study of the bulk Compton spectrum produced by cold plasma accelerating in a blazar jet showed the following results.

(1) If dissipation (i.e. acceleration/injection of relativistic leptons) occurs during the (early) shell acceleration phase, the radiation from the disc can provide a relevant source of photons for the relativistic external Compton process. Broad-line radiation becomes competitive and dominant for such process at a shell–disc distance comparable to the BLR. The dominance between the two components depends on the spectral index of the relativistic Compton spectrum.

(2) The bulk Comptonization of the radiation field originating in the accretion disc produces a component peaking in the far-UV, thus most difficult to observe, and its contribution to the soft X-ray band is negligible.

(3) Instead the bulk Compton scattering of broad-line photons may give an observable feature in the soft X-ray band of the most powerful quasars, if the dissipation takes place close to, but within, the BLR radius when the shell has reached high bulk Lorentz factors (and for small viewing angles).

(4) The transient nature of the bulk Compton feature and the requirement that other radiation processes (most notably, the SSC process) do not dominate over it, imply that the bulk Compton component is rarely detectable. Its absence cannot thus be considered as evidence that jets are not matter dominated.

(5) On the other hand, the detection of this feature allows two key quantities to be estimated: (i) the bulk Lorentz factor, and (ii) the amount of cold leptons in the shell and in turn the corresponding kinetic power.

(6) In principle, the time-dependent behaviour of the bulk Compton component would trace the jet acceleration profile.

(7) The bulk Compton contribution would result in a flattening of the X-ray spectrum towards softer energies, which could mimic absorption, and possibly a hump. Indications of such features have been found in the spectra of some powerful high-redshift blazars. A re-analysis of their X-ray spectra and SED will be presented in a forthcoming paper.

ACKNOWLEDGMENTS

We thank the referee, Rafal Moderski, for his careful reading of this manuscript and his constructive comments, and F. Tavecchio for useful discussions. AC and ACF acknowledge the Italian MIUR and the Royal Society for financial support, respectively.

REFERENCES

Begelman M. C., Sikora M., 1987, ApJ, 322, 650
Begelman M. C., Li Z.-Y., 1994, ApJ, 426, 269
Bentz M. C., Peterson B. M., Pogge R. W., Vestergaard M., Onken C. A., 2006, ApJ, 644, 133
Blandford R. D., 2002, in Gilfanov M., Sunyaev R. et al., eds, Lighthouses of the Universe, ESO Astrophysics Symposia. Springer-Verlag, Berlin, p. 381
Blazejowski M., Siemiginowska A., Sikora M., Moderski R., Bechtold J., 2004, ApJ, 600, L27
Boller T., Fabian A. C., Brandt W. N., Freyberg M. J., 2000, MNRAS, 315, L23
Celotti A., Matt G., 1994, MNRAS, 268, 451
Cohen M. H., Cannon W., Purcell G. H., Shaffer D. B., Broderick J. J., Kellermann K. I., Jauncey D. L., 1971, ApJ, 170, 207
Dermer C. D., Schlickeiser R., 1993, ApJ, 416, 453
Fabian A. C., Celotti A., Iwasawa K., Ghisellini G., 2001a, MNRAS, 324, 628
Fabian A. C., Celotti A., Iwasawa K., McMahon R. G., Carilli C. L., Brandt W. N., Ghisellini G., Hook I. M., 2001b, MNRAS, 323, 373
Fossati G., Maraschi L.Celotti A., Comastri A., Ghisellini G., 1998, MNRAS, 299, 433
Ghisellini G., 1999, Astr. Nach., 320, 232
Ghisellini G., Madau P., 1996, MNRAS, 280, 67
Ghisellini G., Celotti A., Fossati G., Maraschi L., Comastri A., 1998, MNRAS, 301, 451
Ghisellini G., Celotti A., Costamante L., 2002, A&A, 386, 833
Kaspi S., Smith P. S., Netzer H., Maotz D., Iannuzi B. T., Giveon U., 2000, ApJ, 533, 631

Lyutikov M., 2003, New Astron. Rev., 47, 513
Moderski R., Sikora M., Madejski G. M., Kame T., 2004, ApJ, 611, 770
Poutanen J., 1994, ApJS, 97, 607
Rees M. J., 1978, MNRAS, 184, P61
Romani R. W., Sowards-Emmerd D., Greenhill L., Michelson P., 2004, ApJ, 610, L9
Shakura N. I., Sunyaev R. A., 1973, A&A, 24, 337
Sikora M., Madejski G. M., 2000, ApJ, 534, 109
Sikora M., Madejski G. M., Moderski R., Poutanen J., 1997, ApJ, 484, 108
Sikora M., Begelman M. C., Rees M. J., 1994, ApJ, 421, 153
Sikora M., Begelman M. C., Madejski G. M., Lasota J.-P., 2005, ApJ, 625, 72
Spada M., Ghisellini G., Lazzati D., Celotti A., 2001, MNRAS, 325, 1559
Whitney A. R. et al., 1971, Sci, 173, 225
Worsley M. A., Fabian A. C., Celotti A., Iwasawa K., 2004, MNRAS, 350, L67
Worsley M. A., Fabian A. C., Pooley G. G., Chandler C. J., 2006, MNRAS, 368, 844
Yuan W., Fabian A. C., Celotti A., McMahon R., Matsuoka M., 2005, MNRAS, 358, 432
Yuan W., Fabian A. C., Worsley M. A., McMahon R., 2006, MNRAS, 368, 985

This paper has been typeset from a TEX/LATEX file prepared by the author.